DOI: 10.61782/fa.2025.0192

FORUM ACUSTICUM EURONOISE 2025

CHARACTERISATION OF ACOUSTIC METAMATERIALS ALLOWING AIRFLOW

Gianluca Memoli[1*] **Mark Puttock-Brown**[1] **Jonathan Eccles**[3]
Ben Pearce[4] **Emma Greenland**[4]
[1] Department of Informatics, University of Sussex, UK
[2] Department of Engineering, University of Sussex, UK
[3] Metasonixx Ltd, Brighton, UK
[3] Anderson Acoustics, Brighton, UK

ABSTRACT

Managing noise and ventilation at the same time is one of the key challenges for acousticians worldwide. This is why, when a new type of solution – e.g. based on acoustic metamaterials – promises to manage both, it is important to have reliable acoustic and pressure measurements. In this study, we review the applicability of ISO 7235 to three different acoustic metamaterials, based on the principle of phase cancellation. We present acoustic measurements in the lab and benchmark them with measurements taken on a building façade, advocating for a potential revision of the standard. We discuss the challenges of measuring total pressure drop and present a dedicated measurement rig. Our work may be useful to any researcher or acoustician considering the placement of metamaterial-based products in their project.

Keywords: *metamaterials, noise, ventilation, measurements.*

1. INTRODUCTION

In a joint paper from 2022, the UK Association of Noise Consultants and the Institute of Acoustics highlighted the challenges of managing simultaneously noise and ventilation in the built environment [1]. This is because traditional solutions rely on absorbing materials, which are bulky and need to be cleaned periodically, or on mass, which opposes the passage of air, by definition. In this context, different research groups worldwide are looking at acoustic metamaterials as the next candidate for the simultaneous management of noise and ventilation.

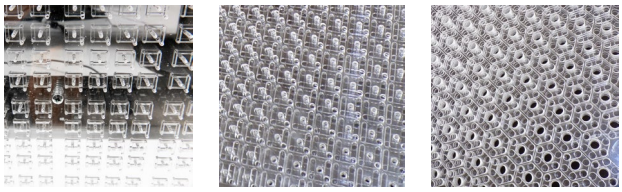

(a) (b) (c)

Figure 1. The three perforated metamaterials of this study, in order of increasing perforated area (ß).

Acoustic metamaterials are a special class of materials, whose acoustic properties are determined by their sub-wavelength geometry, more than their chemical properties [2,3]. Supported by the development of advanced manufacturing, broadband acoustic metamaterials are quickly translating from laboratories to applications. One of the key challenges for acoustic metamaterials, however, is measuring their properties, so that their performance can be compared with more traditional solutions. This is because a solution based on metamaterials is often non-uniform and non-homogeneous: two hypotheses that underpin the most common measurement standards in acoustics (e.g. ISO 10534-2:2023, which relies on impedance tubes [5])

[*] ***Corresponding author***: g.memoli@sussex.ac.uk

Particularly important for ducted silencers and termination units is ISO 7235:2003 [6], which relies on a waveguide to establish flow and allows measurements behind the silencer either in a reverberation room or in a test duct (with anechoic termination) or in "essentially free field" conditions. In this work, we test the validity of this standard to characterize a family of three acoustic metamaterials optimized for transmission loss in the presence of airflow (see Figure 1). We discuss how the challenges of obtaining reliable measurements required dedicated testing rigs – both in acoustic and fluid dynamics – and the need to benchmark potential changes to measurement methods with existing ISO standards.

2. METAMATERIAL DESIGN

The three metamaterials in Figure 1 were fabricated assembling multiple layers. Each layer consists of a 3 mm acrylic sheet, on which unit cells have been excavated in a repetitive pattern (e.g. by laser cutting). Each 2D unit cell is designed to create two paths in the final 3D geometry: a pass-through hole (typically in the center) and a labyrinthine path (typically on the outside). Figure 2 shows the two cases used in this study (a square and a hexagon), both inspired by optical lattices .

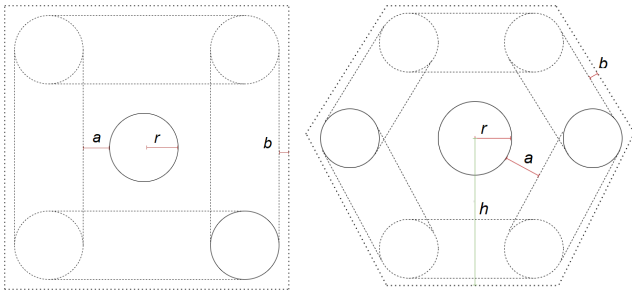

(a) (b)

Figure 2. The unit cells at the base of the metamaterials used in this study.

Different values of the perforation rate ß can be obtained by varying the design parameters of these cells: the radius r of the holes, the spacing a between the central hole and the labyrinth, the radius R of the holes in the labyrinth and the spacing $2b$ between one labyrinthine unit cell and next one. For the square cell (Figure 2a), which has one channel in the center and one on the outside of the same radius (i.e. $R = r$) – the perforation rate $ß_{Square}$ is:

$$\beta_S = \frac{\pi}{2} \cdot \frac{1}{\left(3 + \frac{a+b}{r}\right)^2} \leq 17.4\% \qquad (1)$$

The maximum value in equation (1) is $ß_{Square} \sim \pi/18$, which is obtained when a and b are much smaller than r. In this study, we will be using $ß_1 = 2.5\%$ (two 2 mm diameter holes) and $ß_2 = 6.2\%$ (two 4 mm diameter holes).

The hexagonal unit cell (Figure 2b) has two channels on the outside, for a total of three holes. For even comparison with the square cell, in this study we required the holes in the labyrinth to have the same area as the central hole (i.e. $R = 0.71\ r$), so that the perforation rate is:

$$\beta_H = \frac{2\pi r^2}{\frac{1}{2} \cdot \frac{12}{\sqrt{3}} \cdot h^2} = \sqrt{3}\frac{\pi}{3} \frac{1}{\left(1 + \sqrt{2} + \frac{a+b}{r}\right)^2} \leq 31.1\% \qquad (2)$$

where h is the apothem of the external hexagon. In this study, we used $ß_3 = 12.6\%$ for the hexagon shaped plate.

The acoustic insertion-loss of a hole in a perforated plate, at normal incidence, is due to two contributions: one viscous and one inertial [7]. Using the formulae in [7] we calculated that, for 18 mm thick acrylic plates, the acoustic impedance due to the first term dominates for smaller holes (e.g. microperforated panels), while the second wins as the holes become bigger (∅≥2 mm here) or at larger frequencies (Figure 3).

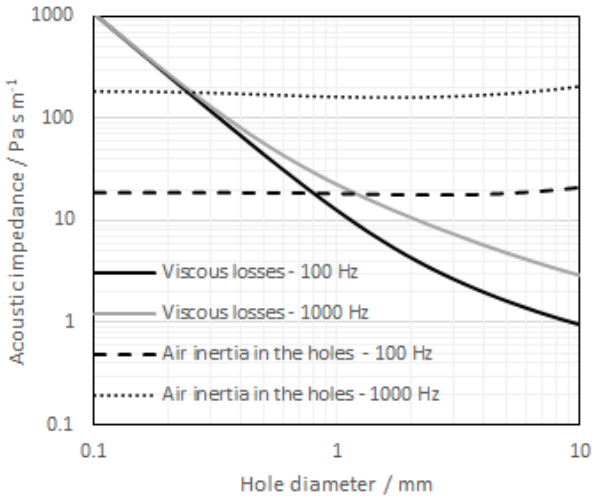

Figure 3. Acoustic impedance for a single hole in an 18 mm thick perforated plate of acrylic as a function of hole diameter and frequency.

(1)

According to Putra and Ismail [7], due to this complex interaction, a perforated plate allows through specific acoustic frequencies with a Lorentzian response, where the center frequency of the Lorentzian (i.e. the frequency with minimal insertion loss) is determined by the size of the holes, by the material of the plate (e.g. density ρ=1180 kg/m^3 and Young modulus E=3 GPa for acrylic) and by the thickness of the plate (t=18 mm for the square plates and t=24 mm for the hexagonal ones). For the 2D unit cells in Figure 2, the length of the (3D) labyrinthine path was designed to cancel the sound that would otherwise go through the central hole (i.e. like a half-wave plate in optics). At first approximation, therefore, the 3D structures originated by the unit cells in Figure 2 combine the broadband insertion loss given by the mass of the layered acrylic plates with the interferometric cancellation between the frequencies going through the two paths [8].

3. ACOUSTIC MEASUREMENTS

In the first instance, the transmission loss of each metamaterial plate was determined starting from the method described in ISO 7235 [6]. A speaker with a metamaterial casing (to remove back-emission – see [9]) was connected to a semi-open cylindrical tube, long enough to provide a planar wavefront for a propagating logarithminc sweep obtained using an arbitrary waveform generator (model RSDG2042X by RS-components) after amplification (model TPA3255 by Fosi audio). Both the speakers used in this part of the study (one for the range 80 Hz – 4000 Hz and one for the range 400Hz – 8000 Hz) had flat frequency response in the range used. ISO 7235 also prescribes to measure the insertion loss using an average over multiple microphone positions. When the measurements are taken in a test duct, the microphones need to be placed along the diagonal of the duct, so that their spacing is at least $\lambda/4$ for each 1/3rd-octave band. In the free-field case, ISO 7235 prescribes microphones to envelope the emission (like in ISO 3746).

In this study, we measured acoustic pressure in essentially free field conditions and calculated the insertion loss as the average over multiple measurements, taken at the exit of the tube with and without the metamaterial plate. The optimal number of microphones and their mutual positions were determined exploiting the traslational symmetry of the metasurface and the guidelines for reducing the number of microphones in acoustic holography (see [10] and references therein). We found that, while three positions were sufficient, they were not supposed to be along a line, so we took a) one measurement along the axis at distance X from the metasurface; b) one measurement off axis, also at a distance X; and c) one measurement off axis, at distance Y from the metasurface. While this method shows some similarities with ISO 7235:2003, a benchmark assessment of the transmission loss was needed.

Figure 3 The metamaterial panel mounted as secondary window by Anderson Acoustics, for the façade measurements.

This was performed by Anderson Acoustics, which used the procedure described in BS EN ISO 16283-3:2016 [11] tipically used for determine the acoustic properties of façade elements. The small square panel ($ß_1$=2.5%) was therefore mounted as secondary window in a standard frame, already containing a PVC window (see Figure 3) A hemi-dodecahedron loudspeaker (Norsonic 250) was used as pink-noise source outside, while a class I, calibrated microphone mounted on a tripod (Norsonic 140) was used to record inside. A potential sound flanking transmission path was identified, via the boiler outlet penetration (see Figure 3), but was neglected due to the mass of the external masonry wall. The window itself was standard thermal double glazing (28 dB Rw+Ctr estimated), with good perimeter seals. The measurement of sound reduction index $D_{ls,2m,nT}$ was performed in two conditions: with the PVC double glazed window open and with the PVC window partially open (i.e. with a 10 cm opening), with and without the metamaterial panel. The results of façade measurements (Figure 4) show a clear effect of the secondary window, whose impact increases with frequency, as expected from a mass-based solution. Once insertion loss was calculated, the results of façade measurements and laboratory tests were found to be similar for $ß_1$=2.5% (Figure 5). The laboratory method was then used for all the other plates (see Table 1).

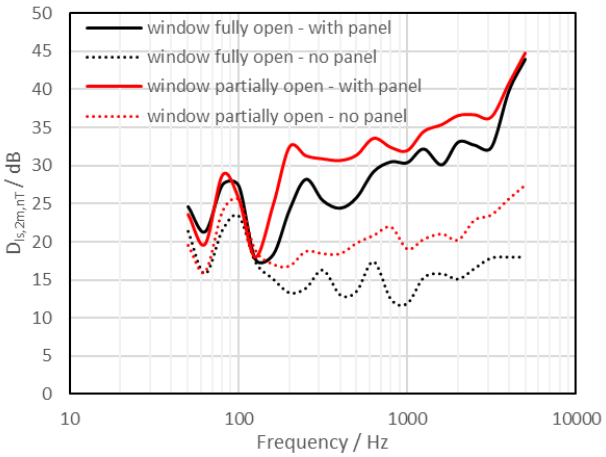

Figure 4 Results of the in-situ acoustic measurements made using the procedure in 16283-3:2016

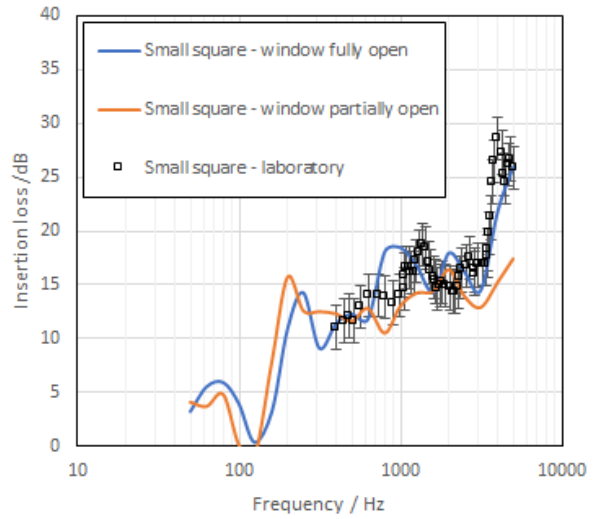

Figure 5 Results of the insertion loss measurements for the metamaterial plate with $ß_1$=2.5%: laboratory tests and façade measurements.

4. PRESSURE DROP MEASUREMENTS

These measurements were conducted using the procedure described in ISO 7235-2: each plate was inserted in the modified square section (hydraulic diameter: D_h = 200 mm) of a suction-type wind tunnel. As shown in Figure 6, each metamaterial plate was secured between two flanges with 12xM8 bolts with a central alignment pin to keep the individual layers in the correct relative orientation. A single-phase axial ventilation fan was positioned downstream of the plate, while upstream the section was extended for 12.2D_h with a square bell mouth to reduce entrance effects. For pressure drop measuring across the plate, two wall mounted pressure tapings were used, whose readings were acquired using an EvoScann P16-D differential pressure scanner. The reference pressure was taken as the ambient atmosphere and measured separately using a precision barometer.

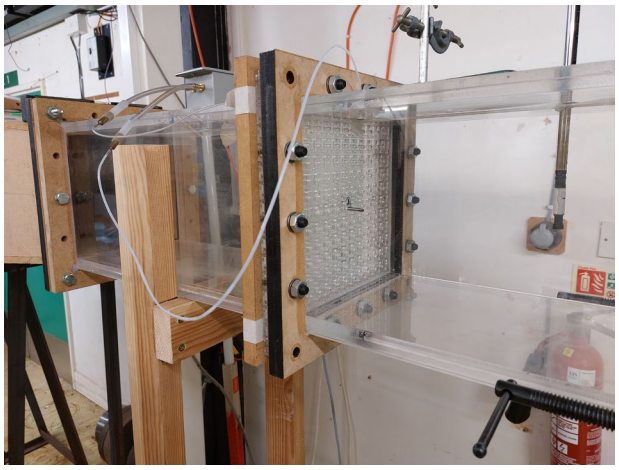

Figure 6 Measurement set-up at Sussex University.

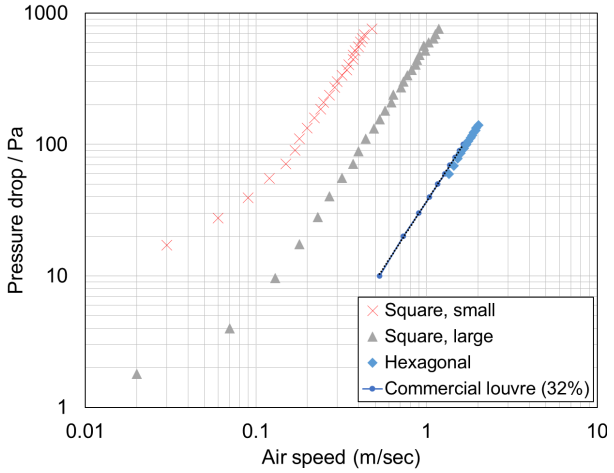

Figure 7 Pressure drop measurements for the three plates in this study and a commercial acoustic louvre.

Volumetric flow rate was measured using a Testo 405i thermal anemometer $10D_h$ from tunnel inlet perpendicular to the flow at the centre over a 30 second average. Given the low flow rate the calculated entrance length to develop a full laminar profile could be up to $1160D_h$ and so a uniform flow in the duct is assumed, and the volumetric flow rate calculated accordingly. Discrete measurement points of pressure drop were obtained by incrementing the fan speed by 100 rpm from 146 (min) to 2800 (max). Figure 7 reports the results of the pressure drop measurements, compared with the pressure drop from the datasheet of a commercial acoustic louvre (model: SlimShield SL-150 by IAC Acoustics, thickness: 150mm thick, weight: 30 kg m^{-2}, effective area: 32%).

5. DISCUSSION

The pressure drop curves in Figure 7 also show the result for a multi-linear fit., with the curve given by the power law:

$$\Delta P = K \cdot v^{\alpha} \tag{3}$$

A multi-linear fit (see Table 1) for velocities above 0.1 m/s gives $\alpha = 2.06 \pm 0.05$, in agreement with Bernoulli's expression which predicts $\alpha=2$ for purely inertial dependence. As shown in Figure 7, the trend deviates from the simple quadratic law for lower velocities, where viscous effects start to dominate, but above 0.1 m/s the constant K corresponds to the total pressure loss coefficient in ISO 7235. The fitting values – $K_1 = 3500 \pm 100$ kg m^{-2} s^{-1} (small squares) $K_2 = 560 \pm 60$ kg m^{-2} s^{-1} (large squares); and $K_3 = 32 \pm 4$ kg m^{-2} s^{-1} (hexagons) – also correspond to the value of the pressure drop at 1 m/s for the three panels. Figure 7 confirms that the pressure drop of the hexagonal panel corresponds to the one of the selected acoustic louvre.

The acoustic measurements show that, in the range 100 – 4000 Hz, the insertion loss of the three panels in Figure 1 follow a similar trend. In Figure 8, we fitted the data with the function [12]:

$$IL = 10 \cdot \log(1 + C \cdot (f - f_0)^{\gamma}) \tag{3}$$

and obtained a similar value for the power law $\gamma = 0.55 \pm 0.5$ where $\gamma = 1$ is expected for a standard mass-based insertion loss. The different values of the constants C (which is related to the surface density of the plate) and f_0 (which is related to the first vibrational thickness mode of each panel) can be found in Table 1.

Table 1. Fitting parameters for the metamaterial panels in Figure 1, as measured in laboratory.

	Small Square	Large square	Hexagon
α	2.02	2.02	2.12
K / kg m^{-2} s^{-1}	3500	560	32
ß / %	2.5	6.2	12.6
γ	0.60	0.50	0.55
C / $Hz^{-\gamma}$	0.38	0.30	0.05
f_0 / Hz	48	78	241
Thickness / mm	18	18	24
Density / kg m^{-2}	16.4	17.6	12.4

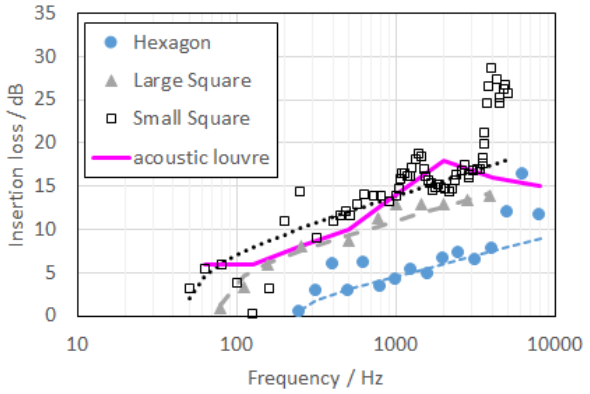

Figure 8 Insertion loss for the panels in Figure 1. The graph also reports the fitting curve from eq. (3) – see Table 1.

According to Figure 8, the acoustic performance of the louvre we selected for comparison falls within the insertion loss of the small square and of the large square. However, 3 dB are lost on average while passing from the Small Square to the large square panel and further 6 dB are lost – on average – while passing from the large square panel to the hexagonal one. This means that, while the hexagonal panel shows the same pressure drop as the selected acoustic louvre, its acoustic attenuation is lower. More work is therefore needed before this type of materials can substitute an acoustic louvre, adding superior acoustic performance to the advantages of less space occupied (24 mm instead of 150 mm) and lower weight (12.4 kg m^{-2} vs 30 kg m^{-2}).

6. CONCLUSIONS

In this work, we characterized three perforated labyrinthine metamaterials using ISO 7235-2. From the fluid dynamic point of view, we highlighted the challenges to run the prescribed measurements and described a dedicated experimental set-up that was built for this purpose at the University of Sussex. From the acoustic point of view, we described the modifications we applied to the standard for having reliable results and the benchmarking procedure followed by Anderson Acoustics using ISO 16283-3.

This study shows how acoustic metamaterials are approaching the performance of traditional solutions, using less space and weight. Like other studies focused on the application of acoustic metamaterials, this work highlighted a design space. Further studies, with more prototypes, will allow us to map the space ($ß$, ΔP, IL) and, consequently, to optimize the design of the panels presented here for specific needs in noise and ventilation management, like silencing heat pumps.

7. ACKNOWLEDGMENTS

The authors GM and MPB acknowledge funding from Research England through the Higher Education Impact Fund, managed by the University of Sussex.

8. REFERENCES

[1] Acoustic Noise Consultants & Institute of Acoustics, "Avoustic Ventilation and Overheating - Residential Design Guide," January 2020. [Online]. Available: https://www.association-of-noise-consultants.co.uk/wp-content/uploads/2019/12/ANC-AVO-Residential-Design-Guide-January-2020-v-1.1.pdf. [Accessed April 2025]

[2] S. Cummer, J. Christensen and A. Alù, "Controlling sound with acoustic metamaterials," *Nature Reviews Materials,* vol. 1, 2016. A. Putra and A. Ismail, "Normal Incidence of Sound Transmission Loss from Perforated Plates with Micro and Macro Size Holes," *Advances in Acoustic and Vibration,* p. article ID 534569, 2014.

[3] C. J. Naify, A. Titovich and M. R. Haberman, "What is an acoustic metamaterial?," in *184th Meeting of the Acoustical Society of America*, Chicago, 2023.

[4] A. A. El Ouahabi and G. Memoli, "A transfer matrix method for calculating the transmission and reflection coefficient of labyrinthine metamaterials," *Journal of the Acoustical Society of America,* vol. 151, p. 1022–1032, 2022.

[5] ISO, "ISO 10534-2: Determination of acoustic properties in impedance tubes. Part 2: Two-microphone technique for normal sound absorption coefficient and normal surface impedance," ISO, Geneva, 2023.

[6] International Standardisation Office, "ISO 7235:2003 - Laboratory measurement procedures for ducted silencers and air-terminal units — Insertion loss, flow noise and total pressure loss," ISO, Geneva, 2003.

[7] A. Putra and A. Ismail, "Normal Incidence of Sound Transmission Loss from Perforated Plates with Micro and Macro Size Holes," *Advances in Acoustic and Vibration,* p. article ID 534569, 2014.

[8] G. Memoli, M. Caleap, D. Sahoo, B. Drinkwater and S. Subramanian, "Acoustic Wave Manipulation". UK Patent WO2018146489A1, 2017.

[9] L. Chisari, P. Martignon, M. Di Cola and G. Memoli, "Preliminary studies for metamaterial based audio systems," in *Proceedings of Euronoise 2021*, 2021.

[10] D. Manwill and J. Blotter, "Nearfield Acoustic Holography Experiments on Variously Correlated Compound Sources," in *SpaceGrant conference*, Salt Lake City, 2009.

[11] ISO, "ISO 16283-3:2016 - Field measurement of sound insulation in buildings and of building elements - Part 3: Facade measurements," ISO, Geneva, 2016.

[12] D. Vigé, "13 - Vehicle interior noise refinement – cabin sound package design and development," in *Vehicle Noise and Vibration Refinement*, Woodhead, 2010, pp. 286-317.